Slow recovery from soil disturbance increases susceptibility of high elevation forests to landslides

Hongxi Liu, Zhun Mao, Yan Wang, John Kim, Franck Bourrier, Awaz Mohamed, Alexia Stokes

RESEARCH ARTICLE

Slow recovery from soil disturbance increases susceptibility of high elevation forests to landslides

Hongxi Liu[1,2], Zhun Mao[3*], Yan Wang[4], John H. Kim[5], Franck Bourrier[6], Awaz Mohamed[7], Alexia Stokes[3]

1. Research and Development Center for Watershed Environmental Eco-Engineering, Beijing Normal University at Zhuhai 519087, China
2. State Key Laboratory of Water Environment Simulation and Pollution Control, School of Environment, Beijing Normal University, Beijing 100875, China
3. Univ Montpellier, AMAP, CIRAD, CNRS, INRAE, IRD, 34000 Montpellier, France
4. XTBG-CAS, Menglun, Mengla, Xishuangbanna, Yunnan, 666303, China
5. Max Planck Institute for Biogeochemistry, Jena, Germany
6. INRAE, 2 Rue de la Papeterie, 38402 Saint-Martin-d'Hères, France
7. Université de Lorraine, AgroParisTech, INRAE, SILVA, F-54000 Nancy, France

Abstract

Natural hazards such as shallow landslides are common phenomena that disturb soil and damage forests. Quantifying the recovery of forest vegetation after a hazard is important for determining the window of susceptibility to new disturbance events, especially at high elevations, where extreme weather events are frequent and the growing season is short. Plant roots can reduce the size of this window on unstable hillslopes, by adding mechanical reinforcement (c_r) to soil and changing its hydrological reinforcement (c_h); data that are used in landslide models to calculate the Factor of Safety (FoS) of a hillslope. We calculated temporal variations in c_r and c_h in naturally regenerated mixed, montane forests in the French Alps. In this closed-canopy forest, open-canopy gaps were present, with understory vegetation comprising herbs, forbs and shrubs. At three altitudes (1400, 1700 and 2000 m), we dug small trenches as proxies for shallow landslide events and calculated c_r before soil disturbance in

both open gaps and closed forest. Then, using monthly tree root initiation and mortality data measured in rhizotrons, we calculated monthly c_r for four years after the disturbance. Temporal FoS was then calculated using an infinite slope stability model.

Results showed that short-lived, ephemeral roots contributed little to soil reinforcement compared to thicker, long-lived roots. After disturbance, mean c_r (over the entire soil profile) never fully recovered to the initial value at any site, although >90% recovery was observed in open gaps at 1400 m. Mean c_r was slow to recover in closed forests, especially at 2000 m, where only 19% recovery occurred after 41 months. The c_h in closed forests was considerable during the summer months, but marked increases in soil water moisture resulted in lower FoS, especially during December to April, when soil was near saturation. As c_r changed little throughout the year, it was a more reliable contributor to slope stability. Our results show therefore, that particular attention should be paid to high elevation forests after a disturbance. Also, during the process of recovery, the highly variable soil water dynamics in closed forest can result in seasonal hotspots of vulnerability. Therefore, when tree transpiration is low, our results highlight a need for careful monitoring on steep or unstable slopes, especially in closed-canopy forests.

*Corresponding author: Z. Mao. E-mail: maozhun04@126.com

Running title: Tree root recovery after disturbance

ACKNOWLEDGEMENTS

We are grateful to the the National Key Research and Development Program of China (2019YFC1510600), Mairie de Chamrousse for access to field sites. Funding was provided by the French and Mexican governments (ECOPICS project, ANR–16-CE03-0009 and CONACYT–2 73659). Thanks are due to B. Marin-Castro (Autonomous National University of Mexico) for descriptions of soil profiles.

DATABASE LINK

Tree root demography data can be freely accessed at: doi.org/10.15454/C3QY4B

Initial root density along intact soil profile data can be freely accessed at: https://doi.org/10.15454/RYMVUS

Forest inventory data can be freely accessed at: https://doi.org/10.15454/JTO5DD

Key words: Fine roots ; mechanical reinforcement; hydrological reinforcement; slope stability; forest gap

71 # 1 INTRODUCTION

72 Landslides are recognized as one of the most dangerous natural hazards that endanger human
73 life and infrastructure in mountainous regions (IPCC, 2012, Petley, 2012). In Europe, the
74 frequency and intensity of shallow landslides triggered by heavy rainfall are predicted to
75 increase (Tichavský et al., 2019). Eco-engineering methods are considered appropriate for
76 improving soil reinforcement and slope stability, through the choice and management of
77 suitable vegetation (Schwarz et al., 2010, Mao et al., 2012, Stokes et al., 2014). Increasing
78 evidence from landslide inventories, experimental and modelling approaches, has shown that
79 reduced forest cover, due largely to disturbances such as tree felling, creates zones that are
80 prone to slope failure (Roering et al., 2003, Mao et al., 2014a, Schwarz et al., 2010, Vergani
81 et al., 2016). High elevation forests are especially susceptible to disturbance and because of
82 the short growing season, take longer to recover than forests at lower elevations (Zhao et al.,
83 2016), but the consequences for soil loss and slope stability are poorly understood. Therefore,
84 forest managers in mountainous regions need more accurate data about the effects of tree
85 removal on slope stability in forests growing at different elevations, as well as the time taken
86 for a slope to recover stability after such disturbance.

87 Vegetation stabilizes soil mechanically through the binding action of thin and fine roots that
88 cross the multiple potential shear (rupture) surfaces along a slope. These roots anchor plants
89 to deeper soil layers (beneath the shear surface) and need to be strong when held under
90 tension. Thicker roots act like soil nails, preventing soil collapse due to their mass, bending
91 strength and stiffness (Greenway, 1987, Stokes et al., 2009). The majority of studies focusing

92 on the contribution of vegetation to slope stability have estimated the number and cross-
93 sectional area (CSA) of roots (<10 mm in diameter) in soil, as well as their tensile strength
94 (see Mao et al., 2012, for a compilation of data). The resulting value is termed the additional
95 cohesion from roots, also known as mechanical cohesion or mechanical reinforcement, and
96 can be used in geotechnical models to calculate a slope's Factor of Safety (FoS, Norris et al.,
97 2008, Greenwood 2006, Thomas and Pollen-Bankhead, 2010, Ji et al., 2012, Mao et al.,
98 2014a). Mechanical reinforcement varies significantly in forests, depending on tree species
99 and size, as well as stand density (Roering et al., 2003, Sakals and Sidle, 2004, Genet et al.,
100 2008, Schwarz et al., 2010, Vergani et al., 2016). Mao et al. (2013) showed that in temperate,
101 montane forests with a closed canopy, mechanical reinforcement was significantly greater
102 than in open-canopy gaps that occurred either through individual tree felling or mortality.
103 This spatial heterogeneity in mechanical reinforcement will therefore impact a slope's overall
104 FoS. Modelling of FoS for forested slopes allows managers to calculate when a slope's
105 mechanical integrity is compromised, and whether practical interventions are necessary. As
106 the FoS is strongly impacted by the number and dimensions of roots crossing the potential
107 shear surface in soil, it is important to determine how forest structure and patchiness affects
108 root growth, but such data are scarce (Mao et al., 2014a, Rossi et al., 2017, Wang et al., 2018).

109 Not only does spatial heterogeneity exist in a forest, but also temporal heterogeneity, as fine
110 roots initiate and then die, usually within several months (Leigh et al., 2002, Wang et al.,
111 2018). Forest age also induces temporal heterogeneity in mechanical reinforcement, as both
112 tree age and species composition (due to successional phase), alter the number, dimensions,

and strength of roots present throughout the soil profile (Sakals and Sidle 2004, Genet et al., 2008, 2010, Vergani et al., 2016). However, these studies have used a synchronic approach, where measurements have been made in stands of different ages, and so do not reflect intra-annual temporal variability. A long-term (>4 years) study estimating mechanical reinforcement in forests has never been performed using a continuous or diachronic approach. The only study examining the short-term (1.5 years) impact of root initiation and growth on mechanical reinforcement (Mao et al., 2013), showed that in temperate, montane forest, once roots had been disturbed through soil excavation, root initiation and growth occurred much faster in open gaps compared to closed forest (Mao et al., 2013). Nevertheless, this study did not take into account variations in precipitation and the intra-annual dynamics of soil water content, that strongly influence the triggering of shallow landslides.

Shallow landslides usually occur when soil is saturated or near saturation (Sidle and Bogaard, 2016). On forested slopes, soil water is removed through plant transpiration and evapotranspiration, increasing soil matric suction (or soil water potential), and improving soil strength (Fredlund and Rahardjo, 1993, Terwilliger, 1990). This increase in soil strength improves slope stability, and as an analogy to mechanical cohesion or reinforcement, has been termed 'hydrological' or 'hydric' cohesion or reinforcement (Greenway, 1987, Fredlund and Rahardjo, 1993, Simon and Collison, 2002, Pollen-Bankhead and Simon, 2010, Veylon et al., 2015, Kim et al., 2017). Hydrological reinforcement has been increasingly investigated under different vegetation covers, either alone (e.g., Hayati et al., 2018a, b) or with mechanical reinforcement (e.g., Simon and Collison 2002, Pollen-Bankhead and Simon 2010, Kim et al.,

2017), and was highly seasonal and strongly linked to climatic events. For example, during the growing season, hydrological reinforcement due to plant transpiration is high and is the main contributor to a slope's FoS (Simon and Collison, 2002, Kim et al., 2017). However, during the winter months or the rainy season, soil is wet and plant transpiration is minimal. Therefore, hydrological reinforcement is low, and a slope's FoS can be reduced to dangerous levels (Kim et al., 2017). Usually, changes in hydrological reinforcement with soil depth are considered using estimated values (Pollen-Bankhead and Simon, 2010), and rarely do studies combine temporal estimations of hydrological reinforcement with seasonal root growth data and their interaction throughout the soil profile (but see Kim et al. 2017). Not only are tree roots initiated throughout the year (with one or two main flushes of growth), but most fine roots die after only a few days, weeks or months (Mao et al., 2013, Wang et al., 2018). To our knowledge, the effect of this root mortality on slope stability throughout the year has never been quantified, but could contribute to seasonal hotspots of vulnerability.

Here, we aim at investigating the intra- and inter-annual variability in reinforcement of slopes recovering from disturbances in open gaps and closed forest at different elevations. Using field data, hydrological reinforcement was estimated and compared with mechanical reinforcement over time. To do this, we integrated existing data from several studies into one geotechnical model that calculated the FoS. These data comprised: (i) root intersection quantity before disturbance (Mao et al., 2012, 2015b) and monthly root initiation and mortality over 4 years (Wang et al., 2018), from which we calculated temporal mechanical reinforcement, (ii) soil mechanical properties and soil water potential (Kim et al., 2017), from

155 which we estimated hydrological reinforcement and (iii) forest inventory data, from which we
156 determined forest structure (Mao et al., 2012, 2015a, 2015b). We hypothesize that the
157 recovery of mechanical reinforcement is affected by forest structure (open-canopy gaps versus
158 closed-canopy forest), altitudes and soil depths and ask: do mechanical and hydrological
159 reinforcement co-vary depending on forest structure and how much does each type of
160 cohesion contribute to the recovery of the slope's FoS?
161

2 MATERIALS AND METHODS

2.1 Study sites

We used data from study sites located near Chamrousse, Isère, in the French Alps (45° 07'N, 5° 52'E). All sites have been studied characterized previously and detailed information can be found in Mao et al., (2015b) and Wang et al., (2018). Sites comprised mixed, mature, naturally regenerated forests growing at altitudes of 1400 m (Prémol forest), 1700 m (Bachat-Bouloud forest) and 2000 m (near Achard Lake, at the treeline). *Abies alba* Mill., *Picea abies* (L.) Karst and *Fagus sylvatica* L. were dominant at 1400 m; *P. abies* and *A. alba* were dominant at 1700 m and *Pinus uncinata* L. was dominant at 2000 m (Mao et al., 2015b). The stand basal area (cross-sectional area of trees at 1.3 m) at 1400 m was in the range of 41-56 m^2 ha^{-1}; 27-33 m^2 ha^{-1} at 1700 m; and 9-19 m^2 ha^{-1} at 2000 m. Mean tree diameter at breast height was 19 cm at 1400 m, 18 cm at 1700 m and 14 cm at 2000 m. With different tree densities, biomass ranges from 29 – 146 t ha^{-1} at different altitudes (Figure S1). Slope angles at the three sites were generally between 10° and 25°, but sometimes could reach 35°.

Climatic data for the three sites were estimated over 2004-2014 using the AURELHY model of Météo-France (Benichou and Le Breton, 1987; Piedallu and Gegout, 2007, 2008, Stokes et al., 2020). The mean monthly air temperature is the lowest in January or February (-2.3 °C at 1400 m; -3.6°C at 1700 m and -5.2 at 2000 m) and highest in July (13.7 °C at 1400 m; 12.0°C at 1700 m; 10.2 °C at 2000 m). Mean annual precipitation is approximately 1500 mm at 1400

m, 1700 mm at 1700 m and 1900 mm at 2000 m. Precipitation amount is highly seasonal, with the lowest amount in summer and highest amount in winter (in the form of snow).

2.2 Soil physical and chemical features

In a separate study, soil features were characterised using profiles and monoliths (0.25 m × 0.25 m) in a nearby transect spanning the same elevational gradient (Table 1, Stokes et al., 2020). Infiltration tests were carried out next to each sampling plot using a constant head single ring infiltrometer and saturated hydraulic conductivity was calculated. Bulk density was determined by taking undisturbed soil cores at different depths within the soil profile. Soil was sieved at 2 mm after air drying and the soil fraction <2 mm was used to assess properties. Soil pH was measured in water as 1:2.5 extract. Soil organic matter (SOM) content was determined via loss-on-ignition at 500 °C (Dean, 1974). Soil texture was determined by laser-diffraction analysis (McCave et al., 1986). The soil sample was previously digested in hydrogen peroxide solution to destroy the organic matter and sodium hexametaphospate to release the bound clay particles.

Soils were acidic at all sites, ranging from (a) “Cambisols (Hyperdystric)” overlying green schist and with an abundant water supply at 1400 m (Joud, 2006), to (b) “Cambisols (Humic, Hyperdystric)” overlying the crystalline formation at 1700 m (Joud, 2006), and to (c) “Epileptic Umbrisols (Hyperdystric)” overlying the crystalline formation at 2000 m (IUSS Working Group WRB, 2007). Soil analyses showed that total carbon content was significantly greater in closed forests than in gaps at both 1700 m and 2000 m, and that SOM was

significantly greater in closed forest compared to gaps at 1700 m. Apart from some slight differences in soil texture at 1700 m and 2000 m, no other differences in soil physicochemical properties were found (Merino-Martín et al., 2020). A seasonal water table existed in open gaps at 1400 m and 1700 m during the winter months. The average maximum rooting depth of soil was approximately 1.0 m at 1400 and 1700 m, but only 0.5 m at 2000 m (Mao et al., 2015b).

2.3 Root demography

We used data describing fine root distribution, the dynamics of root initiation and mortality in paired plots located in open gaps and closed forests at altitudes of 1400, 1700 and 2000 m. These data came from Mao et al., 2013, 2015b and Wang et al., 2018. The three studies used data from the same rhizotrons, but covered different time periods. Mao et al. (2013) started the experiment and installed rhizotrons in the summer of 2009 at 1400 and 1700 m, and 12 months later at 2000 m, and data covered a 1.5 year period. Wang et al. (2018) continued the observations of root growth and mortality until November 2013.

To measure root demography, four trenches were dug at each altitude, two in open gaps and two in closed forest. Rhizotrons were installed by inserting plexiglass sheets against one wall of the trench. Roots were cut during the process, to leave a smooth wall against which to position the plexiglass (Figure S2). Trenches were then covered with wooden boards and corrugated iron. More details on rhizotron installation can be found in Mao et al. (2013). As the installation of rhizotrons disturbed roots and soil in a way similar to that caused during a

221 shallow landslide (e.g., soil crack and detachment and root damage during scarp formation
222 and mass movement), it was considered as a proxy for a landslide event that damages roots
223 around the scarp (Roering et al., 2003), with root growth considered as a recovery process
224 after the disturbance. Initiation and mortality of each root (< 5 mm in diameter) in the
225 rhizotrons was measured monthly, even during the winter months, for a period of 4 years.

226 Three root diameter classes (]0, 1] mm,]1, 2] mm and]2, 5] mm; according to the
227 international standard ISO 31–11,]x, y] denotes a left half-open interval from x (excluded) to
228 y (included)) were differentiated during measurements. Then, root initiation quantity ($I_{i,j}$, in
229 roots m^{-2}), and mortality quantity ($M_{i,j}$, in roots m^{-2}) of diameter class i for j^{th} measurement (j
230 $\in$ [1, J], where J refers to the maximum sequential number of measurement, which differed
231 with altitudes (J = 49 for 1400 m; J = 47 for 1700 m and J = 33 for 2000 m) were counted as a
232 function of soil depth. Net root intersection production of diameter class i for j^{th} measurement
233 (R_{ij}, in roots m^{-2}) and its cumulative form ($C_{i,j}$, in roots m^{-2}) were calculated:

234 $$C_{ij} = \sum_{j=1}^{J} R_{i,j} = \sum_{j=1}^{J} (I_{i,j} - M_{i,j}) \quad \text{(Eq. 1)}$$

235 C_{ij} was used to calculate additional cohesion (or mechanical reinforcement) due to roots after
236 the disturbance event.

237 We used root distribution data from 2009 (Mao et al., 2012, 2015b), that were collected prior
238 to the installation of rhizotrons (the proxy for a soil disturbance event), to estimate the number
239 and diameter of roots in the soil above the bedrock (1.0 m deep at 1400 and 1700 m and 0.5 m
240 deep at 2000 m). Roots were classed into four diameter classes (]0, 1] mm,]1, 2]mm,]2,
241 5]mm,]5, 10]mm). These data enabled us to calculate reference root intersection density,

defined as number of roots of diameter class *i* per unit soil surface at intact soil condition (R_i, in roots m^{-2}). These data were then used as the initial value before disturbance, against which we measured root recovery.

2.4 Hydrological data

Soil hydrological data are from Kim et al. (2017), who performed measurements in our plots. In 2012, four extra trenches were dug (one trench in one open gap, and one in closed forest at each altitude), to measure soil water potential (ψ, kPa) using WaterMark© Granular Matrix sensors, (Irrometer Co., USA). These electrical-resistance type sensors are robust and easy to use. Devices at 2000 m were frequently stolen or damaged, therefore monitoring could not be performed, and due to flooding, periods of data were missing at 1700 m from August 2012 to November 2013, therefore, we only calculated c_h at 1400 m. Each trench was close (< 2.0 m) to a rhizotron to ensure that ψ data could be matched with root demography data. Sensors were installed at different depths (at 0.05, 0.1, 0.2, 0.4, 0.7 m), along a vertical soil profile and data were logged every 30 min from July 2012 to November 2013 (data are from Kim et al., 2017, Fig. S3). Despites some high values of ψ (i.e., >200 kPa, but still within the maximum range of WaterMark sensors), most of the measured values at either of the vegetation types was <150 kPa during our monitoring period (Fig. S3). Merino-Martín et al. (2020) manually measured mean monthly air (0.1 m above soil surface) and soil temperatures (at depths of 0.1 m and 0.4 m) in soil trenches where the rhizotrons were installed, from September 28th, 2010 to March 3rd, 2014 (Figure S4), using a portable thermistor thermometer (HI-93510N Hanna Instruments, USA). Results showed that gaps were slightly warmer than closed forest at all

263 elevations, but significant differences between the two were found only at 1700 m.
264 Temperature at topsoil was more fluctuant than at deep layers, especially at high altitudes of
265 1700 and 2000 m.

266 ***2.5 Cohesion and slope stability***

267 2.5.1 Mechanical reinforcement from roots (c_r)

268 Before slope stability modelling could be performed, it was necessary to calculate mechanical
269 (c_r) and hydrological reinforcement (c_h) from the root intersection production data. c_r was
270 estimated using Wu and Waldron's model (WWM, Wu et al., 1979; Waldron, 1977), which
271 assumes that all roots are mobilized and broken simultaneously, and c_r is provided by the
272 total tensile strength of all roots per soil unit area:

273 $$c_{ri,j} = 1000 R_f \frac{\bar{T}_{ri} \pi \bar{d}_{ri}^2 C_{i,j}}{4 A_S} \quad \text{Eq. (2)}$$

274 where 1000 is the convertor from MPa to kPa, R_f is the root orientation factor, $\bar{T}_{ri}$ is tensile
275 strength of roots of diameter class $\bar{d}_{ri}$, $C_{i,j}$ is cumulative root intersection production as
276 defined in Eq.(1). A_S is the soil area where roots are counted (m^2). $\bar{d}_{ri} \in \{0.5, 1.5, 3.5, d_n\}$
277 corresponding to diameter classes]0, 1] mm,]1, 2] mm,]2, 5] mm and]5, 10] mm. When
278 root diameter >5 mm, we used the actual measured diameter. Roots of >10 mm in diameter
279 were not included in the calculations of soil reinforcement, as the mechanism by which these
280 large diameter roots stabilize slopes is not considered in the cohesion model (Wu et al., 1988).

The choice of WWM was made because it is simple and uses a limited number of parameters. WWM has been widely applied over the last 40 years, so our results can be compared easily with previous studies. It has been shown that WWM overestimates the additional cohesion from roots (Abernethy and Rutherfurd, 2001, Pollen and Simon, 2010). Therefore, we took a corrected coefficient R_f of 0.48 (Preti, 2006), instead of the 1.2 proposed by Wu et al., (1979). Ji et al. (2012) and Mao et al. (2014b) also found that this corrected WWM (Preti, 2006) gave the most conservative c_r, that is comparable to that calculated using Fibre Bundle Models (FBMs), based on force-induced root breakage (Thomas and Pollen-Bankhead, 2010), or displacement-triggered root breakage (Schwarz et al., 2010). Models such as the Root Bundle Model (RBM) (Schwarz et al., 2010) or energy based Fibre Bundle Model (FBM) (Ji et al., 2020) might yield more accurate and realistic c_r, but they require extra data, such as the modulus of elasticity of roots or root rupture energy, that we did not measure in our study.

A power relationship usually exists between root tensile strength (T_{ri}) and root diameter, i.e., $T_{ri} = \alpha \cdot d_i^{\beta}$. Mao et al. (2012) reviewed literature data relating to changes in T_r with root diameter and found that plant functional group had a limited effect on c_r estimation. Therefore, we took a justified generic equation for T_r:

$$T_{ri} = 28.97 \cdot d_i^{-0.52}. \quad \text{Eq. (3)}$$

In order to identify forest patch type (open gaps versus closed forest) and site effects on c_r and how the recovery process possibly changes these effects, we introduced three ratios (R_{1400}, R_{1700}, R_{2000}), which indicated c_r in open gaps divided by c_r in closed forest at altitudes of 1400, 1700 and 2000 m, respectively:

$$R_{1400} = \frac{c_{r,open\ gap,1400m}}{c_{r,closed\ forest,1400m}}$$

$$R_{1700} = \frac{c_{r,open\ gap,1700m}}{c_{r,closed\ forest,1700m}} \quad \text{Eq. (4)}$$

$$R_{2000} = \frac{c_{r,open\ gap,2000m}}{c_{r,closed\ forest,2000m}}$$

When a root tip appeared behind a rhizotron, it started to grow downwards along the plexiglass pane. When the root had branches, whether or not these lateral roots initiated from the main root was uncertain. Therefore, to estimate the range of bias in c_r due to this uncertainty, we performed the following two scenarios in the calculation of c_r. In Scenario A), we included both main and lateral roots; in Scenario B), we excluded lateral roots growing from main roots (Figure S5).

2.5.2 Pore-water pressures: hydrological reinforcement (c_h) and hydrostatic-uplifting force (U_z)

Hydrological reinforcement c_h and hydrostatic-uplifting force U_z were the effects of pore-water pressures on slope stability. When soil is not saturated, negative pore-water pressures produced matric suction and greater shearing resistance, defined as c_h. When soil is saturated, positive pore-water pressures produced hydrostatic-uplifting force, defined as U_z.

We used two different methods proposed by Fredlund et al. (1978) and by Kim et al. (2017), respectively, to calculate c_{h_z} (c_h at zth layer), and chose the more conservative one in data analysis and FoS calculation. First, we used the inverse power-law model between gravimetric soil moisture at zth layer (θ_{g_z}) and c_{h_z}, fitted by Kim et al. (2017). Soil samples were collected from the same study site and were then subject toshear strength test under

different moisture levels to derive soil moisture-shear strength relationships under unsaturated soil condition ($\psi \neq 0$):

$$c_{h_z} = \begin{cases} c_m \theta_{g_z}{}^{-B} - c' & \psi \neq 0 \\ 0 & \psi = 0 \end{cases} \quad \text{Eq. (5)}$$

where, c_m is the apparent maximum soil cohesion at dry condition, B is a fitted reduction coefficient derived, c' is the effective cohesion term subtracted from the unsaturated shear strength term (Kim et al., 2017).

Alternatively, we used the linear equation between c_{h_z} and ψ_z for the soil layer z under unsaturated soil condition (Fredlund et al., 1978, Simon and Collison, 2002):

$$c_{h_z} = \begin{cases} \psi_z tan\phi_b & \psi \neq 0 \\ 0 & \psi = 0 \end{cases} \quad \text{Eq. (6)}$$

where, the angle ϕ_b (in °) represents the conversion rate between tensiometer measured water potential and the hydrological reinforcement. ϕ_b reportedly varied within a narrow range from 10° to 20° (Simon and Collison, 2002). In this study, we took different ϕ_b (5°, 10°, 15°, 20°) to compare c_{h_z} calculated by two methods.

The total c_h of the soil profile was calculated as:

$$c_h = \sum_{k=1}^{K} \frac{c_{h_z} \cdot A_z}{A_S} \quad \text{Eq. (7)}$$

where A_z is the cross-section area of each layer (m^2), A_S is the cross-section area of the profile (m^2).

U_z is calculated as:

$$U_z = \begin{cases} \rho_w g (z_s - z_{sat}) \cos^2(\beta) / 1000 & \psi = 0 \\ 0 & \psi \neq 0 \end{cases} \quad \text{Eq. (8)}$$

where ρ_w is the water density (kg m^{-3}), g is the gravitational acceleration (N kg^{-1}), z_s is the depth of the soil profile (m), z_{sat} is the depth at which soil saturation starts to occur (m), 1000 is to convert Pa to kPa.

2.5.3 Slope stability modelling

Following Kim et al. (2017), we defined the factor of safety (FoS) for each soil layer for a slope with an angle of β (in degree (°)). FoS for the z^{th} soil layer ($z \in Z$; Z is total number of layers), noted as FoS_z (dimensionless) was calculated as the ratio between the stabilizing and destabilizing forces:

$$FoS_z = \frac{c'_z + c_{r_z} + c_{h_z} + \tan\phi_z (\sum_{z=1}^{z} W_z \cos\beta - U_z)}{\sum_{z=1}^{z} W_z \sin\beta} \quad \text{Eq. (9)}$$

where FoS_z determines if the slope at the z^{th} soil layer is safe (FoS ≥1.3), stable but needing monitoring (1.3 >FoS ≥1.0) or not (FoS <1.0); the numerator term is the derived equation of Fredlund et al. (1978), in which both root and hydrological reinforcement were incorporated in the framework of the classical Mohr–Coulomb failure criterion; c'_z, c_{r_z} and c_{h_z} are soil effective cohesion, additional cohesion from roots and hydrological reinforcement of the z^{th} soil layer, respectively (in kPa). c_{h_z}= 0 if soil is saturated (defined as $\psi = 0$). ϕ_z is internal friction angle of (degrees) of the z^{th} layer. W_z is surcharge of soil, water, and biomass of the z^{th} layer per area and accordingly $\sum_{z=1}^{z} W_z$ is the cumulative charge down to the z^{th} layer (kPa). U_z is the hydrostatic-uplifting force, considering that there is a water flow, on the saturated portion of the failure surface (kPa). U_z =0 if soil is not saturated (defined as $\psi \neq 0$).

As suggested in Kim et al., (2017), we used an infinite slope length as a condition for FoS computation, because very long slopes (>500 m) at Chamrousse can commonly be found, therefore W_z was only calculated per unit slope area:

$$W_z = z\gamma_z(1+\theta_g) + B_z = z\gamma_z\left(1+\frac{\theta_v}{\gamma_z}\right) + B_z \quad \text{Eq. (10)}$$

Where, z = soil layer thickness; γ_z = dry bulk soil density (in kN m^3); θ_g and θ_v= gravimetric and volumetric soil water content (dimensionless); B_z= fresh biomass in unit slope area (i.e., tree surcharge, in kPa).

We defined a global *FoS* of the whole slope land as the minimum of FoS_z among all the soil layers

$$FoS = \min(FoS_z) \quad \text{Eq. (11)}$$

Differentiating *FoS* and FoS_z enabled us to assess both slope stability and to identify the effect of the vertical distribution of roots and water on slope stability.

To better facilitate cross-site comparison between mechanical and hydrological reinforcement, the following conditions were set and respected in the modelling of slope stability:

(1) $\beta = 35°$, slope angle was hypothetically fixed to 35° (Kim et al., 2017)

(2) c'_z and ϕ_z of soil at 1400 m was estimated with a shear testing device by Kim et al. (2017). They were fixed as 10 kPa and 40°to soils of different depths and altitudes, respectively.

377 (3) W_z, c_{r_z}, $c_{h_z}$and U_z were calculated for each soil depth. c_{r_z} was calculated for each altitude
378 (1400, 1700, 2000 m); c_{h_z} was calculated for 1400 m based on the available data.

379 (4) B_Z was estimated based on aboveground biomass investigation within forest inventory
380 plots (see Mao et al., 2012, 2015a, 2015b), in which each tree's size and position were
381 measured (see supplementary material for more details).

382 ***2.6 Statistical analyses***

383 One-way analysis of covariance (ANCOVA) was used to test the significance of differences
384 in c_r calculated by two scenarios and c_r between the reference (before disturbance) and the
385 final recovered state (the final measurement in November 2013). Tukey's honestly significant
386 difference (HSD) test was performed when one-way ANCOVA tested for significant
387 differences with p <0.05. Analysis of variance (ANOVA) was used to calculate contribution
388 of factors (altitude, forest patch type, soil depth, root diameter and monthly interval) to the
389 variability of root production, mortality, living root numbers, and the c_r recovery after
390 disturbance. Data were transformed to meet a normal distribution when necessary. All
391 statistical analyses were performed with R version 3.4.3 ((http://www.r-project.org/).
392

393 **3 RESULTS**

394 ***3.1 Root initiation and mortality***

Initiation and mortality of roots were highly seasonal (Figure S6-S8) and were significantly and positively correlated in all plots (Figure 1, Table S1), especially in the]0, 1] mm diameter class. Roots in the]1, 2] mm and]2, 5] mm diameter classes had very high rates of initiation compared to rates of mortality. Root diameter and soil depth best explained the variation in root initiation quantity, I_{ij}, with contributions of 11% and 10%, respectively (Table 2). Root diameter also explained 20 % and 19% of the variability in root mortality quantity, M_{ij}, and cumulative net root intersection C_{ij}, respectively, whereas soil depth only explained 5% and 7%, respectively (Table 2). Altitude and patch type (open gaps versus closed forest) were both significant and explained more variation in I_{ij} (3.1% and 4.5%, respectively) than M_{ij} (1.5% and 2.5%, respectively) and C_{ij} (2.2% and 2.5%, respectively). Although temporal effects were significant, time since disturbance explained poorly the variation in I_{ij}, M_{ij} and C_{ij} (Table 2), suggesting that much of the variation may be seasonally driven.

3.2 Recovery of mechanical reinforcement (c_r) after the disturbance event

Before the disturbance, mean c_r (over the whole soil profile) in open gaps was lower than that under closed forest at 1400 m (R_{1400_before} = 0.55) and 1700 m (R_{1700_before} = 0.54), but at 2000 m, mean c_r in open gaps was similar to that in closed forest (R_{2000_before} = 1.10; Table 4). After the disturbance, mean c_r in open gaps was almost twice that in closed forest at 1400 m (R_{1400_after} = 1.94), whereas differences between open gaps and closed forest decreased after the disturbance event at 1700 m (ratio increased from 0.54 to 0.90, Table 4).

When c_r was calculated using the two different scenarios (A: all roots included and B: branched roots excluded), results were similar at all altitudes, soil depths and in each forest patch type (Figure 4), therefore, the scenario used had little effect on the results.

Mean c_r had not fully recovered to its initial value before disturbance, at any of the sites or altitudes, by the end of the study period (Figure 2). Four years after disturbance, c_r had recovered by over 90% (in open gaps) and 26% (in closed forests) at 1400 m, and by 46% (in open gaps) and 28% (in closed forest) at 1700 m (Table 3). However, at 2000m, c_r had only recovered by 23% (in open gaps) and 19% (in closed forest) after 41 months (Table 3).

Mean c_r recovery was more dependent on root diameter than spatial or time factors (Table 2). Before disturbance, roots in the]>2 mm] contributed >50% to c_r at all altitudes (in both open gaps and closed forests). However, after the disturbance event, roots in the]> 5] mm class diameter never appeared. Roots in the]2, 5] mm were not the primary contributor to c_r at most sites and in some cases, (i.e. in open gaps at 1700 m and closed forests at 1400 m), contributed equally or slightly more than]1, 2] mm roots. Instead, roots in the]1, 2] mm class diameter became the major contributor to c_r.

3.3 Vertical distribution of mechanical reinforcement (c_r) before and after the disturbance event

At all sites, before the disturbance event, c_r was highest in the top 0.2 m and then decreased with increasing soil depth. At all sites and altitudes, there were significant differences in c_r before and after the disturbance event, with c_r decreasing significantly in the topsoil (0.0 – 0.2

m) after the disturbance (Figure 4). After disturbance, c_r in the top 0.2 m layer never recovered more than 40% at any site, but deeper in the soil, c_r recovered to >50% of the initial value at all sites and altitudes (except at 2000 m) (Figures 3, S9, S10). The fastest recovery in c_r occurred at a depth of 0.8 – 1.0 m in open gaps at 1400 m, and after only 12 months, c_r was four times greater than the value before the disturbance event (Table 3).

3.4 Seasonal variability in mechanical reinforcement (c_r) and hydrological reinforcement (c_h)

After the disturbance event, mean c_r (over the whole soil profile) increased linearly, then flattened out over time. Except for open gaps at 1400 m, the first winter caused a decreased increment in mean c_r, or delayed the appearance of root initiation in periods with snow cover, compared to those without (Figure 2). No obvious seasonal variability was observed in c_r.

Mean hydrological reinforcement (c_h) calculated using the method in Fredlund et al. (1978), was much higher than that calculated using the method from Kim et al. (2017), where ϕ_b fell in the range 10° – 20° (Simon and Collison, 2002). However, when $\phi_b = 5°$, c_h calculated using Fredlund et al. (1978) was close to that calculated using Kim et al. (2017) (Figure S11). Because Kim et al. (2017) derived soil moisture-shear strength relationships based on soil samples from our study sites, we used c_h from Kim et al. (2017) for analyses and FoS calculation. c_h varied significantly through the year (Figure 2), regardless of site or depth in the soil (Figure 3). Hydrological reinforcement was lowest in winter and spring (i.e., from December to April), but was close to, or was higher, than mean c_r in summer (i.e., from May to November, Figures 2, 3).

3.5 Slope stability

At 1400 m, 3 months after the disturbance event, the rapid increase in mean c_r in open gaps started to significantly improve slope stability, increasing FoS by over 25% (Figure 5a). However, although mean c_r in closed forest was lower than in open gaps, due to the seasonal changes in mean c_h, FoS was similar between closed forest and open gaps during the summer months (Figure 5a, b). Mean c_h contributed to the FoS more than mean c_r in closed forest, although it was highly seasonal and could even be absent (Figure 5b). Soil was occasionally close to saturation or was saturated, usually during the periods of snow cover, and so the hydrostatic-uplifting force slightly decreased FoS (Figure 5). Affected by mean c_h, FoS showed strong seasonal patterns with lower values during the winter. The FoS was less influenced by the c_r and c_h values that were estimated at depths of 0.6 – 1.0 m in the soil (Figure S12). Greater contributions of mean c_r to FoS in open gaps compared to closed forest were also observed at 1700 m and 2000 m (Figures S13, S14).

4 DISCUSSION

4.1 Recovery of mechanical reinforcement (c_r): effects of elevation, patch and depth in soil

Consistent with our hypothesis, once the soil disturbance event had occurred, the recovery of mean c_r to its initial value was more rapid in open gaps than closed forest (Table 3). At 1400 m, over 90% of c_r had recovered after 4 years in open gaps, but only 26% had recovered in the closed forest. However, this difference lessened with increasing altitude: at 1700 m, c_r

475 recovered by almost 50% in the open gaps but less than 30% in the closed forest. At the
476 highest elevation (2000 m), in both open gaps and closed forest, the lack of production of
477 thicker roots meant that c_r recovered by less than 25%, even after 41 months. As the growing
478 season at this altitude is usually only 5 – 8 months (Wang et al., 2018), presumably it would
479 take several years before thicker root production could match those found at lower altitudes,
480 where the growing season is 7 – 10 months (Wang et al., 2018).

481 Several reasons exist to explain the faster recovery of root production in open gaps at lower
482 elevations. Closed forests at 1400 m were significantly denser with larger trees than at the
483 higher altitudes (Figure S1). Therefore, root systems are probably extensive and extend
484 further into open gaps than at higher elevations. Morphological differences exist between
485 open gaps and closed forests, resulting in a greater quantity of solar irradiance and water that
486 reach the understory and soil in open gaps, positively impacting root growth (Coates and
487 Burton 1997, Brett and Klinka 1998). At the same field sites as in our study, Merino-Martín et
488 al. (2020) showed that at elevations of 1400 m and 1700 m, mean negative soil water potential
489 was greater (soil was drier) under closed forest compared to open gaps, but that soil physical
490 and chemical properties were similar (apart from soil carbon that was greater under closed
491 forest at higher elevations). Therefore, microclimate may be influencing root elongation but
492 not soil properties. It is now well documented that soil temperature is a major driver of root
493 growth in temperate forests (Mao et al., 2013, Germon et al., 2016, Mohamed et al., 2017,
494 Wang et al., 2018). The slightly warmer soil in open gaps compared to closed forests may
495 have accelerated c_r recovery in open gaps compared to closed forests. But if this was the case,

this phenomenon should be more obvious at 1700 m, where open gaps were significantly warmer than closed forest. It seems more likely that as coarse roots present in open gaps are distal to the tree, they will be thinner and have a greater potential for recovery after wounding (Stokes et al., 2009). Compared to proximal roots, distal roots also have greater quantities of non-structural carbohydrate (NSC, Wang et al., 2018). NSC is produced during photosynthesis and typically comprises mobile soluble sugars and large, non-mobile, granular starch, that can be mobilized for fast growth after wounding (Hoch et al., 2003). Therefore, distal roots have a better recovery rate than proximal roots.

With regard to different soil depths, c_r recovery in the topsoil (0.0 – 0.2 m) was poor and reached only 40% of the initial value before the disturbance event (at all sites). However, deeper in the soil, c_r recovered by over 50% at 1400 and 1700 m. In the open gaps at 1400 m, c_r at a depth of 0.8 – 1.0 m reached over six times the initial value. Reasons for this disparity in c_r recovery with soil depth may be found in the way that roots respond to the local soil climate. Root elongation is usually slower in topsoil than deeper in the soil because it is less buffered against abrupt changes in air temperature and precipitation (Mohamed et al., 2020). In general, topsoil is colder and more humid in the winter and warmer and drier in the summer compared to the deeper layers, where temperature and soil moisture are less variable (Waisel et al., 2002). We also found that this was true at our study site (Figure S4). Snowmelt may also increase the formation of frost in topsoil, hindering root growth and causing mortality (Tierney et al., 2001). However, although root elongation in topsoil was less than in the deeper layers, in terms of resistance to landslides, where mechanical reinforcement is

517 required deeper in the soil, there will be little effect of surface roots on a slope's factor of
518 safety.

519 ***4.2 Recovery of mechanical reinforcement (c_r): effect of root diameter***

520 Mean c_r recovery (over the whole soil profile), was dependent on root diameter, and roots in
521 the 1 – 2 mm and 2 – 5 mm diameter classes were the main contributors to c_r after disturbance.
522 We suggest that c_r recovery follows the "maximum efficiency" rule of root production, i.e.,
523 more resources are required to construct thicker roots than fine roots (Kitajima et al., 2010;
524 Valenzuela-Estrada et al., 2008). This rule also states that under suboptimal growth conditions,
525 plants initially build 'low-cost' fine roots (0 – 2 mm) to create a transport pathway for
526 resource provision, in order to then reach "maximum efficiency," in terms of growth and
527 functioning. We observed that the finest roots (0 – 1 mm diameter) were the first to be
528 initiated after the disturbance, followed by those in the 1 – 2 m diameter class, and finally by
529 those in the 2 – 5 mm diameter class (Figure 1). Similar results were also found in the grass
530 species, *Zea mays,* during the winter (Barlow and Rathfelder, 1985), but data for woody
531 species are rare. However, these very fine 'low-cost' roots also had a high turnover, and
532 therefore were of an ephemeral nature. The function of these very fine roots would be to
533 quickly explore soil and forage for resources in the short growing season, before being 'shed'
534 by the tree (Wang et al., 2018). Due to this high turnover, very fine roots therefore contribute
535 little to c_r after disturbance. As these very fine ephemeral roots were rapidly initiated after
536 disturbance, but contributed little to c_r, we estimated that at 1400 m and 1700 m, it took 1.3 –
537 1.6 years before longer-lived and thicker roots were produced. However, at 2000 m, c_r never

538 returned to the original value during the 3.5 years of monitoring, underlining the fragility of
539 these subalpine forests when exposed to disturbance.

540 Including branched roots or not, into the calculation of c_r did not change results significantly
541 (Figure 4). Therefore, although rhizotrons may induce artefacts because they force roots to
542 grow against the plexiglass window (Joslin and Wolfe, 1999), they did not impact the
543 calculation of mean c_r.

544 ***4.3 Which type of reinforcement contributes more to slope stability?***

545 Although root initiation and mortality were strongly affected by season, mean cumulative c_r
546 (i.e., regardless of soil depth), increased continuously until a stable state was reached.
547 However, distinct fluctuations in hydrological reinforcement (c_h), controlled by pore-water
548 pressure (Terwilliger, 1990), were noted in all open gaps and closed forest, as well as soil
549 depths, as also observed by others (Pollen-Bankhead and Simon, 2010, Kim et al., 2017,
550 Hayati et al., 2018a). During the winter months, soil moisture is high and can be saturated
551 from precipitation and snow, and water uptake by dominant plants is minimal. Low c_h in both
552 open gaps and closed forests also supported the findings of previous studies that the effects of
553 vegetation on soil hydrologic conditions could be neglected during dormant season (Pollen-
554 Bankhead and Simon, 2010, Hayati et al., 2018a). During the spring, despite the physiological
555 activities of vegetation that increase evapotranspiration, snowmelt leads to high soil moisture
556 and even saturation (Hayati et al., 2018a). Reduced c_h, and extra uplifting force during soil
557 saturation increases the likelihood of shallow landslides. However, during the summer (June –

August), plant transpiration increases, drying the soil and making negative pore-water pressure lower and c_h higher, often to levels similar to or greater than c_r (Figure 3). As for differences in c_h between closed forest and open gaps, higher c_h in forest stands compared to areas lacking a canopy, has already been observed, largely because of rainfall interception by the canopy, or root water uptake (Simon and Collison, 2002, Hayati et al., 2018a). Although c_h is high in the summer, mechanical reinforcement from roots is more stable throughout the year, and is therefore a more reliable contribution to slope stability.

Our results were slightly different from a previous study at the same site, that showed a smaller impact of c_r on FoS (Kim et al., 2017). This difference in results was because Kim et al. (2017), used data commencing 2.5 years after rhizotron installation to calculate c_r. Therefore, root growth had already recovered significantly after the disturbance. Our results also demonstrate a net disparity in the calculation of c_h depending on the method used (Eq. (6) from Fredlund et al., (1978) versus Kim et al. (2017)'s empirical model). We esteem that Kim et al. (2017)'s model using c_h and soil moisture was more reliable, as the model used experimental data from all plots. Also, c_h calculated using the method from Kim et al. (2017) provided more conservative values than c_h using Eq. (6) where an arbitrary choice of the ϕ_b can cause major variations in c_h. Such a comparison highlights the utmost importance of properly choosing ϕ_b values for c_h estimation when Fredlund et al., (1978)'s method is used.

4.4 How does disturbance and recovery of roots affect slope stability?

577 Compared to the summer months, slope stability decreases in the winter, due not only to the
578 low contribution of c_h, but also because of the rising water table in deeper soil layers. Once
579 soil is saturated because of a high water table, the decrease in FoS could be exacerbated due
580 to the water uplifting force (Simon and Collison, 2002). In our study, a seasonal water table
581 was only observed in gaps at 1400 m and 1700 m, not in closed forest. Therefore, gaps could
582 become vulnerable in winter due to such a hydrological process, highlighting the importance
583 of the mechanical role of tree roots on slope stability.
584
585 The rapid recovery of root production and growth is important for reducing the window of
586 landslide susceptibility after a disturbance. We showed that this recovery was fastest in open
587 gaps growing at the lowest elevation (1400 m). In closed forests, there were more roots
588 initially, as well as the presence of coarse root systems, binding and nailing soil in place.
589 However, c_r recovery was poor, particularly deeper in the soil. To reinforce a slope, it is
590 important that the contribution from c_r is high deeper in the soil where the potential shear
591 zone is likely to be located (Stokes et al., 2009). As a result, after soil disturbance, slopes
592 under closed forests at 1400 m and 1700 m had a lower FoS than in open gaps, except during
593 the summer, when c_h was high, but this is the time of year when precipitation-induced
594 landslides are minimal in this region. Our results show therefore that very dense closed forests
595 have higher resistance, but lower resilience than open gaps, when subjected to disturbances
596 that can cause root mortality. The presence of very dense, closed forest around small gaps
597 (<625 m²), also hastens root recovery in gaps, especially at lower elevations where
598 temperatures are warmer. Therefore, high elevation forests, with small, sparsely distributed

599 trees, have a lower resilience to soil disturbance, increasing the window of susceptibility to
600 landslides and natural hazards.

601 Including our study, most modelling work on the effects of vegetation and/or water on FoS
602 have been based on the paradigm of Mohr–Coulomb failure criterion, in which the
603 contributions of vegetation and water to shear resistance are considered as cohesion terms (c_r
604 and c_h) juxtaposed with the soil's effective cohesion (c') (Simon and Collison, 2002, Pollen-
605 Bankhead and Simon, 2010, Kim et al., 2017). Such a simplification greatly enhances the
606 model's applicability, as c_r and c_h, along with c', can be measured or modelled separately
607 prior to their incorporation to the Mohr–Coulomb failure criterion. However, to what extent
608 such a paradigm reflects real soil-root biophysical processes is uncertain, especially as the
609 impact of large roots on slope stability are not considered. Although we show that slope
610 stability can be temporarily compromised in closed forests once a disturbance event has
611 occurred, we did not include the effect of large roots in our model, even though they were
612 always present and will significantly improve slope stability (Nakamura et al., 2007,
613 Giadrossich et al., 2019). Therefore, although our results provide useful information on the
614 recovery of root growth after a disturbance event, and the impact for cohesion over time, a
615 simple comparison of safety factors between open gaps and closed forest must be performed
616 with care. Similarly, comparisons of different types of vegetation on slope stability, based on
617 results from models using only data on fine roots should be assessed with caution. The
618 development of a robust slope stability model that integrates all root size classes with soil and
619 water, as well as their interactions, is now a priority.

5 Conclusions

We show that after a soil disturbance event, distinct differences occurred in the recovery of root initiation and growth in open gaps and closed forests at different elevations. Mean mechanical reinforcement (over the whole soil profile) never fully recovered to the value before the disturbance. However, in open gaps, mechanical reinforcement at depths of 0.8 – 1.0 m recovered after 12 months at elevations of 1400 m and 24 months at 1700 m. In closed forests, recovery took 48 months at the same depth. In forests at 2000 m, root initiation and growth were minimal after the disturbance and only recovered by 25% of the initial value, even after 41 months. Therefore, these high elevation forests are particularly vulnerable to disturbance. Although mechanical reinforcement under closed forests was higher than that in gaps before disturbance, the recovery after disturbance was slow, compromising slope stability for at least 4 years. Such distinct effects of elevation and forest patchiness should be considered by managers working in landslide prone areas. Regarding the type of cohesion, we demonstrate that hydrological reinforcement due to transpiration and drying of soils was high during the summer, particularly in the closed forests. However, during the winter months, when soil was saturated and transpiration was minimal, hydrological reinforcement was negligible. The mechanical effects of roots on soil cohesion was much more stable throughout the year, and increased over the years following disturbance. Therefore, hydrological reinforcement contributed little to long-term slope stability, and mechanical reinforcement from roots was a much more reliable contributor to slope stability.

641 **REFERENCES**

642 Abernethy, B., Rutherfurd, I.D. (2001). The distribution and strength of riparian tree roots in relation
643 to riverbank reinforcement. *Hydrological Processes,* 15(1): 63 – 79. https://doi.org/10.1002/hyp.152

644 Barlow, PW,, Rathfelder, EL. (1985). Cell division and regeneration in primary root meristems of *Zea*
645 *mays* recovering from cold treatment. *Environmental and Experimental Botany*, 25: 303 – 314.
646 https://doi.org/10.1016/0098-8472(85)90028-0

647 Benichou, P., Le Breton. (1987). Prix Nobert Gerbier 1986: prise en compte de la topographie pour la
648 cartographie des champs pluviométriques statistiques. *Météorologie (Paris. 1925)*, 19: 28

649 Brett, RB., Klinka, K. (1998). A transition from gap to tree-island regeneration patterns in the
650 subalpine forest of south-coastal British Columbia. *Canadian Journal of Forest Research,* 28:1825 –
651 1831. doi: 10.1139/x98-160

652 Coates, KD., Burton, PJ. (1997). A gap-based approach for development of silvicultural systems to
653 address ecosystem management objectives. *Forest Ecology and Management,* 99:337 – 354.
654 https://doi.org/10.1016/S0378-1127(97)00113-8

655 Dean, W.E. (1974). Determination of carbonate and organic matter in calcareous sediments and
656 sedimentary rocks by loss on ignition; comparison with other methods. *Journal of Sedimentary*
657 *Research,* 44(1): 242 – 248. https://doi.org/10.1306/74D729D2-2B21-11D7-8648000102C1865D

658 Fredlund, D.G., Morgenstern, N.R. and Widger, R.A. (1978). The shear strength of unsaturated soils.
659 Canadian geotechnical journal, 15(3): 313 – 321. https://doi.org/10.1139/t78-029

660 Fredlund, D.G., Rahardjo, H. (1993). Soil Mechanics of Unsaturated Soils. John Wiley and Sons, New
661 York.

662 Genet, M., Kokutse, N., Stokes, A., Fourcaud, T., Cai, X.H., Ji, J.N., Mickovski, S. (2008). Root
663 reinforcement in plantations of *Cryptomeria japonica* D. Don: effect of tree age and stand structure on
664 slope stability. *Forest Ecology and Management,* 256:1517 – 1526. doi: 10.1016/j.foreco.2008.05.050

665 Genet, M., Stokes, A., Fourcaud, T., Norris, J.E. (2010). The influence of plant diversity on slope
666 stability in a moist evergreen deciduous forest. *Ecological Engineering,* 36:265 – 275.
667 https://doi.org/10.1016/j.ecoleng.2009.05.018

668 Germon, A., Cardinael, R., Prieto, I., Mao, Z., Kim, J., Stokes, A., Dupraz, C., Laclau, J., Jourdan, C.
669 (2016). Unexpected phenology and lifespan of shallow and deep fine roots of walnut trees grown in a
670 silvoarable Mediterranean agroforestry system. *Plant and Soil,* 401: 409 – 426. doi: 10.1007/s11104-
671 015-2753-5

672 Giadrossich, F., Cohen, D., Schwarz, M., Ganga, A., Marrosu, R., Pirastru, M., and Capra, G. F.
673 (2019). Large roots dominate the contribution of trees to slope stability. *Earth Surface Processes and*
674 *Landforms,* 44: 1602 – 1609. https://doi.org/10.1002/esp.4597

675 Greenway, D. (1987). Vegetation and slope stability, in Slope Stability: Geotechnical Engineering and
676 Geomorphology, edited by M. Anderson and K. Richards, pp. 187 – 230, John Wiley, Chichester, U.
677 K.

678 Greenwood, J.R. (2006). SLIP4EX – a program for routine slope stability analysis to include the
679 effects of vegetation, reinforcement and hydrological changes. In: Stokes, A., Spanos, I., Norris, J.E.,
680 Cammeraat, E. (Eds.), Eco- and Ground Bio-Engineering: The Use of Vegetation to Improve Slope
681 Stability, 103. Springer, Dordrecht, pp. 193 – 202.

682 Hayati, E., Abdi, E., Saravi, M.M., Nieber, J.L., Majnounian, B., Chirico, G.B., Wilson, B., Nazarirad,
683 M. (2018a). Soil water dynamics under different forest vegetation cover: Implications for hillslope
684 stability. *Earth Surface Processes and Landforms,* 43: 2106 – 2120. https://doi.org/10.1002/esp.4376

685 Hayati, E., Abdi, E., Saravi, M.M., Nieber, J.L., Majnounian, B., Chirico, G.B. (2018b). How deep can
686 forest vegetation cover extend their hydrological reinforcing. *Hydrological Processes,* 32: 2570 –
687 2583. https://doi.org/10.1002/hyp.13174

688 Hoch G, Richter A, Körner C (2003). Non structural carbon compounds in temperate forest trees.
689 *Plant, Cell & Environment,* 26: 1067 – 1081. https://doi.org/10.1046/j.0016-8025.2003.01032.x

690 IPCC, (2012). Summary for Policymakers. In: Managing the Risks of Extreme Events and Disasters to
691 Advance Climate Change Adaptation [Field, C.B., V. Barros, T.F. Stocker, D. Qin, D.J. Dokken, K.L.
692 Ebi, M.D. Mastrandrea, K.J. Mach, G.-K. Plattner, S.K. Allen, M. Tignor, and P.M. Midgley (eds.)]. A
693 Special Report of Working Groups I and II of the Intergovernmental Panel on Climate Change.
694 Cambridge University Press, Cambridge, UK, and New York, NY, USA, pp. 1 – 19.

695 IUSS Working Group WRB, 2007: World Reference Base for Soil Resources (2006). First Update
696 2007. Rome: FAO, World Soil Resources Reports No. 103.

697 Ji, J.N., Kokutse, N., Genet, M., Fourcaud, T., Zhang, Z.Q. (2012). Effect of spatial variation of tree
698 root characteristics on slope stability. A case study on Black Locust (*Robinia pseudoacacia*) and
699 Arborvitae (*Platycladus orientalis*) stands on the Loess Plateau, China. *Catena*. 92: 139 – 154.
700 doi:10.1016/j.catena.2011.12.008

701 Ji, J., Mao, Z., Qu, W. and Zhang, Z. (2020). Energy-based fibre bundle model algorithms to predict
702 soil reinforcement by roots. *Plant and Soil*, *446*(1): 307 – 329. DOI: 10.1007/s11104-019-04327-z

703 Joud, D. (2006). Guide pour identifier les stations forestières de Rhône-Alpes—Synthèse pour les
704 Alpes du Nord et les montagnes de l'Ain. CRPF Rhône-Alpes, pp 132

705 Joslin, J.D. and Wolfe, M.H. (1999). Disturbances during minirhizotron installation can affect root
706 observation data. *Soil Science Society of America Journal*, 63: 218 – 221.
707 https://doi.org/10.2136/sssaj1999.03615995006300010031x

708 Kim, J. H., Fourcaud, T., Jourdan, C., Maeght, J.L., Mao, Z., Metayer, J., Meylan, L., Pierret, A.,
709 Rapidel, B., Roupsard, O., de Rouw, A., Sanchez, M.Y., Wang, Y., Stokes, A. (2017). Vegetation as a
710 driver of temporal variations in slope stability: The impact of hydrological processes. *Geophysical*
711 *Research Letters,* 44(10): 4897 – 4907, doi:10.1002/2017GL073174.

712 Kitajima K, Anderson KE, Allen MF. (2010). Effect of soil temperature and soil water content on fine
713 root turnover rate in a California mixed conifer ecosystem. *Journal of Geophysical Research*, 115:
714 G04032. doi:10.1029/2009JG001210.

715 Leigh, M.B., Fletcher, J.S., Fu, X., Schmitz, F.J. (2002). Root turnover: an important source of
716 microbial substrates in rhizosphere remediation of recalcitrant contaminants. *Environmental Science*
717 *Technology,* 36(7): 1579 – 83. https://doi.org/10.1021/es015702i.

718 Merino-Martín, L., Griffiths, R.I., Gweon, H.S., Furget-Bretagnon, C., Oliver, A., Mao, Z., Bissonnais,
719 Y.L., Stokes, A. (2020). Rhizosphere bacteria are more strongly related to plant root traits than fungi
720 in temperate montane forests: insights from closed and open forest patches along an elevational
721 gradient. *Plant and Soil,* 450 :183 – 200. doi: 10.1007/s11104-020-04479-3

722 Mohamed, A., Stokes, A., Mao, Z., Jourdan, C., Sabatier, S., Pailler, F., Fourtier, S., Dufour, L.,
723 Monnier, Y. 2017. Linking above- and belowground phenology of hybrid walnut growing along a
724 climatic gradient in temperate agroforestry systems. *Plant and Soil*, 424:103 – 122.
725 https ://doi.org/10.1007/s1110 4-017-3417-4

726 Mohamed A., Monnier Y., Mao Z.,, Jourdan C., Sabatier S., Pailler F., Fourtier S., Dufour L., Millan
727 M., Stokes A. (2020). Shoot and root phenological relationships in hybrid walnut growing in a
728 Mediterranean alley cropping system. *New Forests*, 51:41 – 60

729 Mao, Z., Saint-André, L., Genet, M., Mine, F., Jourdan, C., Rey, H., Courbaud, B., Stokes, A. (2012).
730 Engineering ecological protection against landslides in diverse mountain forests: choosing cohesion
731 models. *Ecological Engineering*, 45: 55 – 69. https://doi.org/10.1016/j.ecoleng.2011.03.026.

732 Mao, Z., Jourdan, C., Bonis, M.L., Pailler, F., Rey, H., Saint-André, L., Stokes, A. (2013). Modelling
733 root demography in heterogeneous mountainous forests and applications for slope stability analysis.
734 *Plant and Soil*, 363: 357 – 382. doi: 10.1007/s11104-012-1324-2.

735 Mao, Z., Bourrier, F., Stokes, A., Fourcaud, T. (2014a). Three-dimensional modelling of slope
736 stability in heterogeneous montane forest ecosystems. *Ecological Modelling*, 273: 11 – 22.
737 https://doi.org/10.1016/j.ecolmodel.2013.10.017.

738 Mao, Z., Yang, M., Bourrier, F. and Fourcaud, T., (2014b). Evaluation of root reinforcement models
739 using numerical modelling approaches. *Plant and soil*, *381*(1 – 2): 249 – 270. doi: 10.1007/s11104-
740 014-2116-7

741 Mao, Z., Saint-André, L., Bourrier, F., Stokes, A., Cordonnier, T., (2015a). Modelling and predicting
742 the spatial distribution of tree root density in heterogeneous forest ecosystems. *Annals of Botany,* 116,
743 261 – 277. https://doi.org/10.1093/aob/mcv092

744 Mao, Z., Wang, Y., Jourdan, C., Cécillon, L., Nespoulous, J., Rey, H., Saint-André, L., Stokes, A.
745 (2015b). Characterizing above- and belowground carbon partitioning in forest trees along an
746 altitudinal gradient using area-based indicators. *Arctic, Antarctic, and Alpine Research,* 47:1, 59 – 69,
747 doi: 10.1657/AAAR0014-014

748 McCave, I.N. (1986). Local and global aspects of the bottom nepheloid layers in the world ocean.
749 *Netherlands Journal of Sea Research,* 20(2 – 3): 167 – 181. https://doi.org/10.1016/0077-
750 7579(86)90040-2

751 Nakamura H., Nghiem Q.M., Iwasa N. (2007). Reinforcement of tree roots in slope stability: A case
752 study from the Ozawa slope in Iwate Prefecture, Japan. In: Stokes A., Spanos I., Norris J., Cammeraat
753 L.H. (Eds) 'Eco- and Ground Bio-Engineering: The Use of Vegetation to Improve Slope Stability.'
754 Developments in Plant and Soil Sciences vol. 103, Springer, Dordrecht. p81 – 90.

755 Norris, JE., Stokes, A., Mickovski, SB., Cammeraat, LH., van Beek, LPH., Nicoll, BC., Achim, A.
756 (eds) (2008). Slope stability and erosion control: ecotechnological solutions. Springer, Dordrecht, pp
757 290

758 Petley, D. (2012). Global patterns of loss of life from landslides, *Geology,* 40(10): 927 – 930.
759 https://doi.org/10.1130/G33217.1

760 Piedallu, C., Gégout, J.C. (2007). Multiscale computation of solar radiation for predictive vegetation
761 modelling. *Annals of forest science,* 64: 899 – 909. DOI: 10.1051/forest:2007072

762 Piedallu, C., Gégout, J.C. (2008). Efficient assessment of topographic solar radiation to improve plant
763 distribution models. *Agricultural and Forest Meteorology,* 148(11): 1696 – 1706.
764 https://doi.org/10.1016/j.agrformet.2008.06.001

765 Pollen-Bankhead, N., Simon, A. (2010). Hydrologic and hydraulic effects of riparian root networks on
766 streambank stability: Is mechanical root-reinforcement the whole story? *Geomorphology,* 116: 353 –
767 362. doi:10.1016/j.geomorph.2009.11.013

768 Preti, F. and Schwarz, M. (2006). On root reinforcement modelling, The role of vegetation in slope
769 stability and mitigation measures against landslides and debris flows, EGU General Assembly, 2 – 7
770 April 2006, *Geophysical Research Abstract,* 8, 04555

771 Roering, JJ., Schmidt, KM., Stock, JD., Dietrich, WE., Montgomery, DR. (2003). Shallow landsliding,
772 root reinforcement, and the spatial distribution of trees in the Oregon Coast Range. *Canadian*
773 *Geotechnical Journal*, 40: 237 – 253. https://doi.org/10.1139/t02-113

774 Rossi, L., Rapidel, B., Roupsard, O., Villatoro-sánchez, M., Mao, Z., Nespoulous, J., Perez, J., Prieto,
775 I., Roument, C., Metselaar, K., Schoorl, J.M., Claessens, L., Stokes, A. (2017). Sensitivity of the
776 landslide model LAPSUS_LS to vegetation and soil parameters. *Ecological Engineering*, 109, 249 –
777 255. https://doi.org/10.1016/j.ecoleng.2017.08.010

778 Sakals, M.E., Sidle, R.C. (2004). A spatial and temporal model of root cohesion in forest soils.
779 *Canadian Journal of Forest Research*, 34(4): 950 – 958. https://doi.org/10.1139/x03-268.

780 Schwarz, M., Preti, F., Giadrossich, F., Lehmann, P., Or, D. (2010). Quantifying the role of vegetation
781 in slope stability: a case study in Tuscany (Italy). *Ecological Engineering,* 36:285 – 291.
782 https://doi.org/10.1016/j.ecoleng.2009.06.014.

783 Sidle, R. C., and Bogaard, T. A. (2016). Dynamic earth system and ecological controls of rainfall-
784 initiated landslides. *Earth Science Review*, 159: 275 – 291.
785 https://doi.org/10.1016/j.earscirev.2016.05.013

786 Simon, A., Collison, A.J.C. (2002). Quantifying the mechanical and hydrologic effects of riparian
787 vegetation on streambank stability. *Earth Surface Processes and Landforms,* 27: 527 – 546.
788 https://doi.org/10.1002/esp.325.

789 Stokes, A., Atger, C., Bengough, A.G., Fourcaud, T., Sidle, R.C. (2009). Desirable plant root traits for
790 protecting natural and engineered slopes against landslides. *Plant and Soil*, 324:1 – 30.
791 doi:10.1007/s11104-009-0159-y

792 Stokes, A., Douglas G., Fourcaud T., Giadrossich F., Gillies C., Hubble T., Kim J.H., Loades K., Mao
793 Z., McIvor I., Mickovski S.B., Mitchell S., Osman N., Phillips C., Poesen J., Polster D., Preti F.,
794 Raymond P., Rey F., Schwarz M., Walker L.R. (2014). Ecological mitigation of hillslope instability:
795 ten key issues facing researchers and practitioners. *Plant and Soil,* 377: 1 – 23.
796 http://dx.doi.org/10.1007/s11104-014-2044-6

797 Stokes A., Angeles G., Barois I., Bounous M, Cruz-Maldonaldo N, Decaëns T, Freschet G., Gabriac Q,
798 Hernandez D., Jimenez L., Ma J, Mao Z, Marin-Castro B, Merino-Martin L, Mohamed A, Reverchon
799 F, Selli L., Sieron K., Weemstra M., Roumet C (2020). Shifts in soil and plant functional diversity
800 along an altitudinal gradient in the French Alps. *BMC Research Notes*. Submitted

801 Terwilliger, V.J., (1990). Effects of vegetation on soil slippage by pore pressure modification. *Earth*
802 *Surface Processes and Landforms*, 15: 553 – 570. doi: 10.1002/esp.3290150607

Tierney GL, Fahey TJ, Groffman PM, Hardy JP, Fitzhugh RD, Driscoll CT. (2001). Soil freezing alters fine root dynamics in a northern hardwood forest. *Biogeochemistry*, 56: 175 – 190. doi: 10.1023/A:1013072519889

Tichavský, R., Ballesteros-Cánovas, J.A., Šilhán, K., Tolasz, R., Stoffel, M. (2019). Dry spells and extreme precipitation are the main trigger of landslides in central Europe. *Scientific Reports,* 9: 14560. https://doi.org/10.1038/s41598-019-51148-2.

Thomas, R.E., Pollen-Bankhead, N., (2010). Modeling root-reinforcement with a fiber-bundle model and Monte Carlo simulation. *Ecological Engineering*, 36: 47 – 61. https://doi.org/10.1016/j.ecoleng.2009.09.008

Valenzuela-Estrada, LR., Vera-Caraballo, V., Ruth, LE., Eissenstat, DM. (2008). Root anatomy, morphology, and longevity among root orders in *Vaccinium corymbosum* (Ericaceae). *American Journal of Botany*, 95: 1506 – 1514. doi:10.3732/ajb.0800092

Vergani, C., Schwarz, M., Soldati, M., Corda, A., Giadrossich, F., Chiaradia, E.A., Morando, P., Bassanelli, C. (2016). Root reinforcement dynamics in subalpine spruce forests following timber harvest: a case study in Canton Schwyz, Switzerland. *Catena*, 143: 275 – 288. https://doi.org/10.1016/j.catena.2016.03.038.

Veylon, G., Ghestem, M., Stokes, A., Bernard, A. (2015). Quantification of mechanical and hydric components of soil reinforcement by plant roots. *Canadian Geotechnical Journal,* 52(11): 1839 – 1849. doi: 10.1139/cgj-2014-0090

Waldron, L.J., (1977). The shear resistance of root-permeated homogeneous and stratified soil. *Soil Science Society of America Journal*, 41: 843 – 848. doi:10.2136/sssaj1977.03615995004100050005x

Wang, Y., Kim, J.H., Mao, Z., Ramel, M., Pailler, F., Perez, J., Rey, H., Tron, S., Jourdan, C., Stokes, A. (2018) Tree root dynamics in montane and sub-alpine mixed forest patches. *Annals of Botany,* 00:1 – 12. doi: 10.1093/aob/mcy021.

Waisel Y, Eshel A, Beeckman T, Kafkafi U (2002). Plant roots: the hidden half. CRC Press, Boca Raton, USA.

Waldron, L.J. (1977). The shear resistance of root-permeated homogeneous and stratified soil. *Soil Science Society of America Journal*, 41(5): 843 – 847. https://doi.org/10.2136/sssaj1977.03615995004100050005x

Wu, T.H., McKinnel, W.P., Swanston, D.N., (1979). Strength of tree roots on Prince of Wales Island, Alaska. *Canadian Geotechnical Journal*, 16 (1), 19 – 33. https://doi.org/10.1139/cgj-2017-0344.

834 Wu, T.H., Beal, P.E., Lan, C., (1988). In-situ shear test of soil–root systems. *Journal of Geotechnical*
835 *Engineering*, 114: 1376 – 1394. DOI: 10.1061/(ASCE)0733-9410(1988)114:12(1376)

836 Zhao, F.R.; Meng, R.; Huang, C.; Zhao, M.; Zhao, F.A.; Gong, P.; Yu, L.; Zhu, Z. (2016). Long-term
837 post-disturbance forest recovery in the Greater Yellowstone ecosystem analyzed using Landsat
838 Time Series Stack. *Remote Sensing,* 8: 898. doi: 10.3390/rs8110898

TABLES

Table 1 Physical and chemical soil properties at different altitudes at the study site (from Stokes et al., 2020).

Altitude (m)	Soil depth (cm)	Clay-silt-sand (%)	Organic carbon content (%)	Bulk density (g cm^{-3})	Mean saturated hydraulic conductivity (cm h^{-1})	FAO soil type
2000	0-30	29-44-27	5.1	1.5	12.73	Histic Hyperskeletic Cambisol (Turbic)
	30-50	13-40-47	1.9	1.3		
1700	0-20	36-41-23	15.1	1.4	19.04	Histic Orthoskeletic Cambisol (Loamic, Turbic)
	20-40	26-45-29	7.4	1.6		
	40-80	18-44-37	6.5	1.6		
	80-100	15-48-37	6.8	1.8		
1400	0-20	28-49-23	13.5	1.5	10.09	Someric Histic Umbrisol (Turbic)
	20-40	13-48-39	2.7	1.1		
	40-60	8-42-50	1.3	1.2		
	60-80	11-44-45	1.9	1.2		
	80-100	9-44-47	2.4	1.2		

In the dataset from Stokes et al., (2020), soil samples were taken from a nearby transect along the slope, at depths of 0-7 cm, 7-25 cm, 25-40 cm, 40-65 cm, 65-77 cm, 77-92 cm at 1400 m; at depths of 0-14 cm, 14-45 cm, 45-76 cm, 76-97 cm at 1600 m; and at depths of 0-30 cm, 30-54 cm at 2000 m. We used the soil properties measured at 1600 m to represent those at 1700 m in this study.

Table 2 Results of two-way ANCOVA test on the effects of spatial (altitude, patch, soil depth), biological (root diameter) and temporal factors on the recovery process of root initiation quantity (I_{ij}, m^{-2}), root mortality quantity (M_{ij}, m^{-2}), cumulative net root intersection production (C_{ij}, m^{-2}) and mechanical reinforcement (c_r, kPa). Asterisks indicate significant correlations (where, ***, $p < 0.001$). Numbers in bold indicate the highest contributions (%).

Factor	**Root initiation quantity (I_{ij}, in m^{-2}),**		**Root mortality quantity (M_{ij}, in m^{-2}),**		**Cumulative net root intersection (C_{ij}, in m^{-2})**		**Mechanical reinforcement (c_r in kPa)**	
	F	Contribution (%)	F	Contribution (%)	F	Contribution (%)	F	Contribution (%)
Altitude	146.08***	3.10	70.98***	1.52	104.05***	2.18	8.47***	0.18
Patch (open gap/closed forest)	426.29***	4.52	231.65***	2.47	236.75***	2.48	159.04***	1.73
Soil depth	247.22***	**10.48**	124.63***	5.32	162.30***	6.80	202.54***	8.81
Root diameter	517.40***	**10.97**	912.81***	**19.50**	892.90***	**18.71**	771.07***	**16.76**
Time (month)	5.35***	0.62	3.02***	0.36	2.87***	0.33	3.51***	0.42
Residuals	NA	70.31	NA	70.84	NA	69.49	NA	72.10

Table 3. Ratio between mechanical reinforcement (c_r) before and after the soil disturbance event. The table was filled with different background colours depending on the ratio: red in the range]0, 0.25], orange in the range]0.25, 0.5], blue in the range]0.5, 1.0], green in the range]>1.0].]0, 12],]12, 24],]24, 36],]36, 48]and]48, 53] represent the five periods of recovery since disturbance.

Altitude	Depth (cm)	Open gap					Closed forest				
		]0, 12]	]12, 24]	]24, 36]	]36, 48]	]48, 53]	]0, 12]	]12, 24]	]24, 36]	]36, 48]	]48, 53]
2000	0-20	0.09	0.28	0.37	0.39#	-	0.09	0.23	0.27	0.29#	-
	20-40	0.21	0.51	0.56	0.58#	-	0.43	0.44	0.47	0.49#	-
	40-50	0	0.01	0.01	0.01#	-	0.00	0	0	0#	-
	Average	**0.07**	**0.20**	**0.22**	**0.23#**	-	**0.06**	**0.16**	**0.17**	**0.19#**	-
1700	0-20	0.03	0.20	0.24	0.27	0.28	0.06	0.07	0.09	0.11	0.12
	20-40	0.15	0.55	0.65	0.73	0.75	0.15	0.29	0.32	0.37	0.40
	40-60	0.20	0.62	0.75	1.03	1.06	0.12	0.39	0.73	1.06	1.19
	60-80	0.15	0.64	0.68	0.79	0.81	0.09	0.40	0.94	1.82	2.12
	80-100##	0.35	1.10	1.48	1.48	1.48	-	-	-	-	
	Average	**0.09**	**0.33**	**0.39**	**0.44**	**0.46**	**0.08**	**0.14**	**0.18**	**0.25**	**0.29**
1400	0-20	0.13	0.14	0.14	0.15	0.16	0.02	0.05	0.07	0.10	0.12
	20-40	0.97	1.09	1.14	1.16	1.18	0.10	0.20	0.26	0.31	0.33
	40-60	1.99	2.32	2.49	2.51	2.51	0.07	0.18	0.24	0.43	0.48
	60-80	1.86	2.75	3.03	3.08	3.08	0.03	0.10	0.16	0.44	0.56
	80-100	4.21	5.40	6.40	6.59	6.65	0.08	0.35	0.47	1.06	1.12
	Average	**0.71**	**0.82**	**0.88**	**0.90**	**0.91**	**0.05**	**0.11**	**0.15**	**0.22**	**0.26**

[#] Rhizotrons at 2000m were installed 12 months later than 1400 and 1700 m, therefore the observation time at 2000 m lasted 41 months, not 48 months.

[##] No roots were observed at 0.8 – 1.0 m in the closed forest at 1700 m, so there were no corresponding data (-).

Table 4 Effects of patch (open gaps and closed forest) at different altitudes (1400, 1700 and 2000 m) on mechanical reinforcement (c_r) before and after the disturbance. R_{1400}, R_{1700} and R_{2000} indicate the ratios of c_r between open gaps and closed forests at 1400, 1700 and 2000 m, respectively (see Eq. (4))

Soil depth (m)	R_{1400}		R_{1700}		R_{2000}	
	Before	After	Before	After	Before	After
0.0 – 0.2	0.58	0.79	0.47	1.11	1.27	1.37
0.2 – 0.4	0.54	1.91	0.60	1.08	1.00	1.16
0.4 – 0.6	0.48	2.42	0.94	0.82	0.92	-
0.6 – 0.8	0.57	3.08	0.82	0.32	-	-
0.8 – 1.0	0.45	2.59	-	1.41	-	-
Total	0.55	1.94	0.54	0.90	1.10	1.16

FIGURE CAPTIONS

Figure 1 Root initiation quantity and mortality quantity in open gaps and closed forests from different root diameter classes at (a,b) 2000 m, (c,d) 1700 m, (e,f) 1400 m. Root diameter classes are indicated in subscript in the legend and represented by: (a,c,e) squares ($R_{0\text{-}1}$ for roots]0,1] mm), (b,d,f) triangles ($R_{1\text{-}2}$ for roots]1,2] mm) and circles ($R_{2\text{-}5}$ for roots of]2,5] mm). When root initiation quantity and mortality quantity were significantly correlated ($p < 0.01$), regression lines were plotted (see Table S1 for equations) for data from open gaps (dashed lines, filled symbols) and closed forests (solid lines, empty symbols).

Figure 2 Mechanical reinforcement (c_r) due to roots of different diameter classes before and after disturbance in (a, c, e) open gaps and (b, d, f) closed forests, at different altitudes (1400, 1700 and 2000 m) from 2009 to 2014. Triangles indicate hydrological reinforcement monitored from July 2012 to November 2013. The horizontal line corresponds to the initial c_r prior to the disturbance; the arrow indicates the time when the disturbance occurred. The grey background indicates the time when the soil surface was covered by snow.

Figure 3 Mechanical reinforcement (c_r) due to roots of different diameter classes before and after the disturbance in: (a, c, e, g, i) open gaps and (b, d, f, h, j) closed forests at different soil depths (every 0.20 m) at an altitude of 1400 m. Triangles indicate hydrological reinforcement monitored from July 2012 to November 2013. The horizontal line corresponds to the reference level; the arrow indicates the time when the disturbance occurred. The grey background indicates the time when the soil surface was covered by snow.

Figure 4 Vertical distribution of mechanical reinforcement (c_r) due to roots before and 4 years after the disturbance at 1400 and 1700 m in open gaps (a and c) and closed forests (b and d). c_{r1} and c_{r2} indicated two scenarios: including branched roots or not, respectively, into the c_r

892 calculation after the disturbance. There were no significant differences between altitudes and
893 between patch types (open gaps versus closed forests). Data are means ± standard error.

894 Figure 5 Global factor of safety (FoS) of slopes in open gaps and closed forests at 1400 m
895 during the monitoring period (2009 – 2014). Each component of FoS is shown where soil load,
896 water load and biomass correspond to W_Z in Eq. (9); soil cohesion corresponds to $\frac{c_z^{'}}{W_Z sin\beta}$ in Eq.
897 (9), which was obtained from root free direct soil shear tests and is given as 3.0 kPa; mechanical
898 and hydrological reinforcement correspond to $\frac{c_{r_z}}{W_Z sin\beta}$ and $\frac{c_{h_z}}{W_Z sin\beta_{h_z}}$ in Eq. (9), respectively;
899 hydrostatic-uplifting corresponds to U_Z in Eq. (9), which gives a negative value to FoS when
900 soil is saturated. The arrow indicates the time when the soil moisture was included. FoS > 1.3
901 indicates that the slope is stable; 1 < FoS < 1.3 the slope is safe but should be monitored and
902 FoS < 1 is an unstable slope. The grey background indicates the time when the soil surface
903 was covered by snow.

904 Figure 1

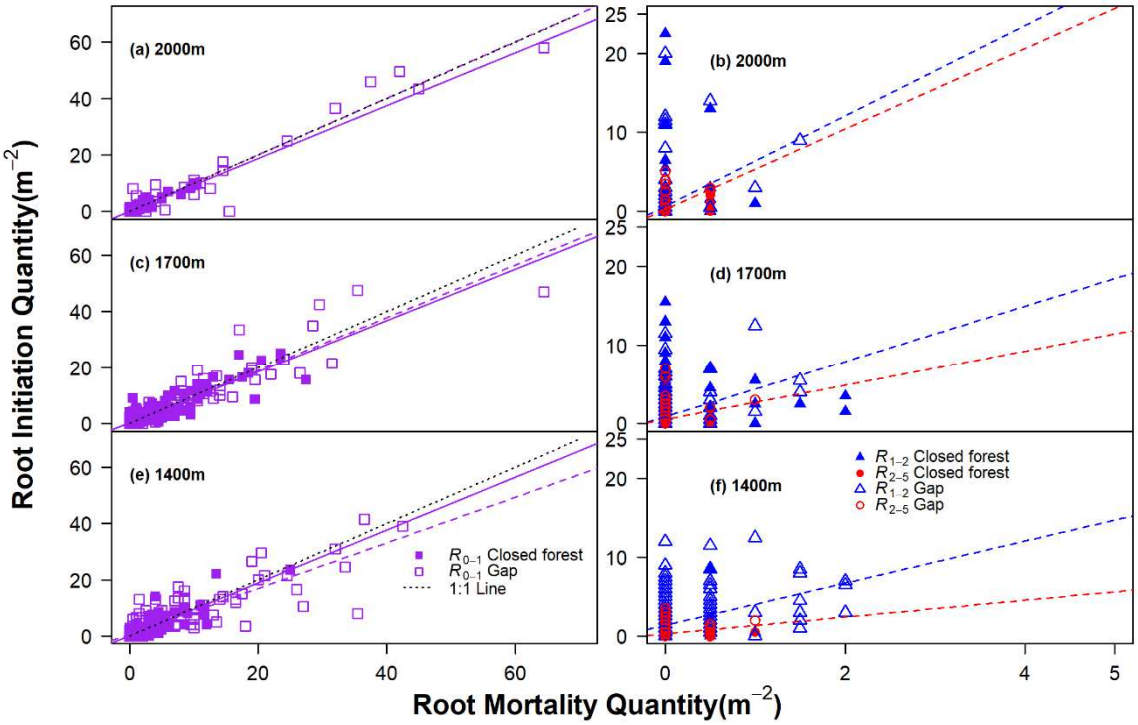

905

906 Figure 2

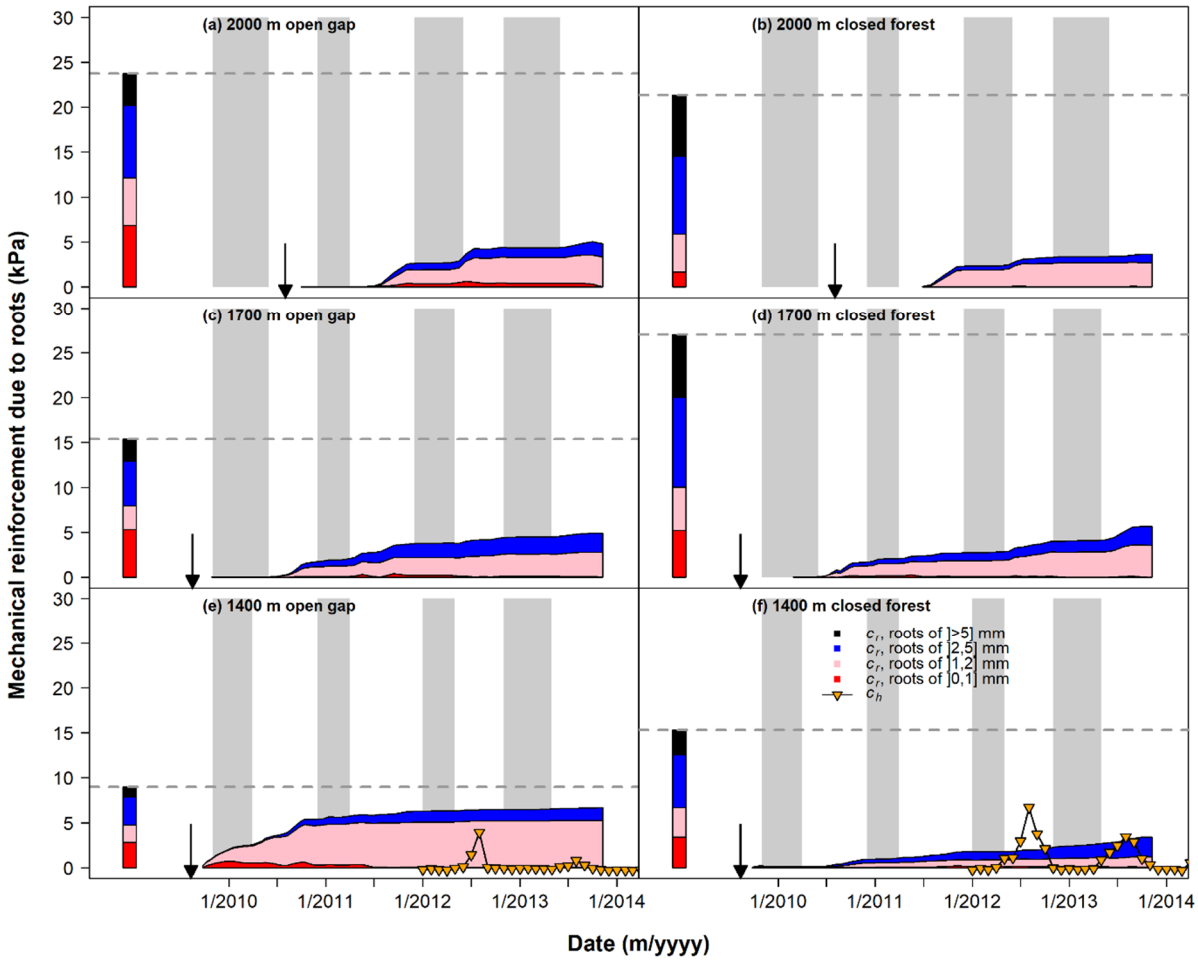

907

908 Figure 3

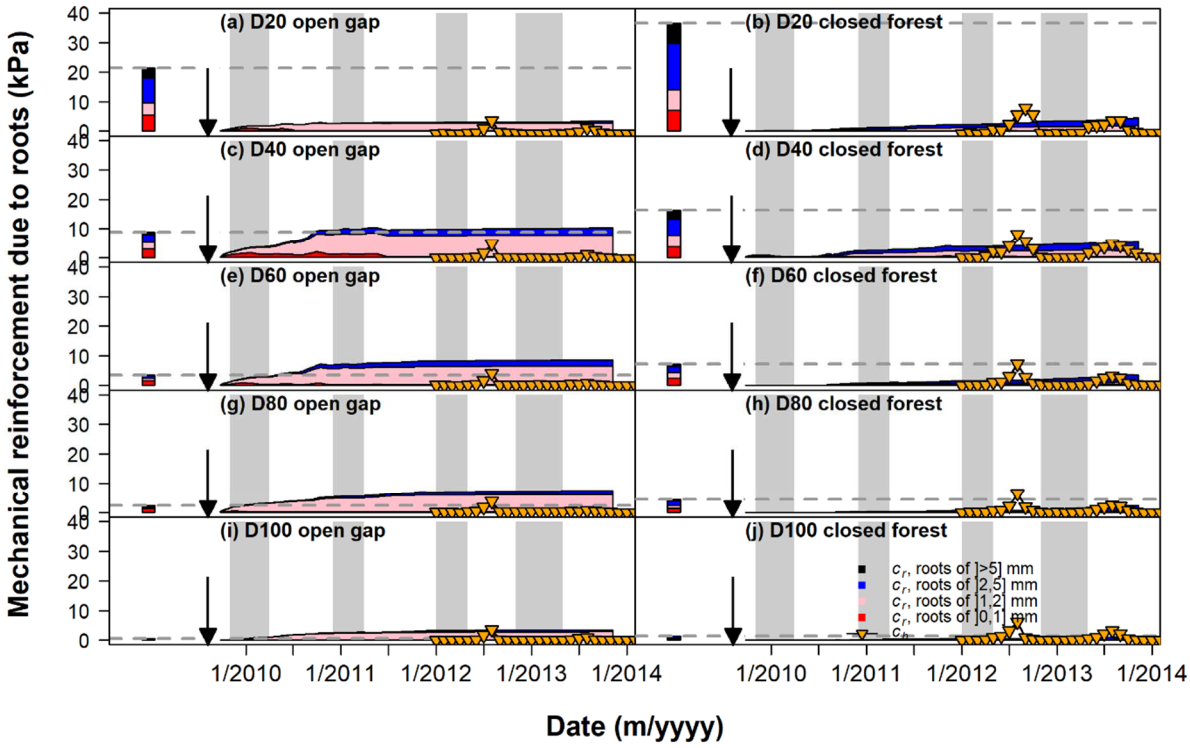

909

910 Figure 4

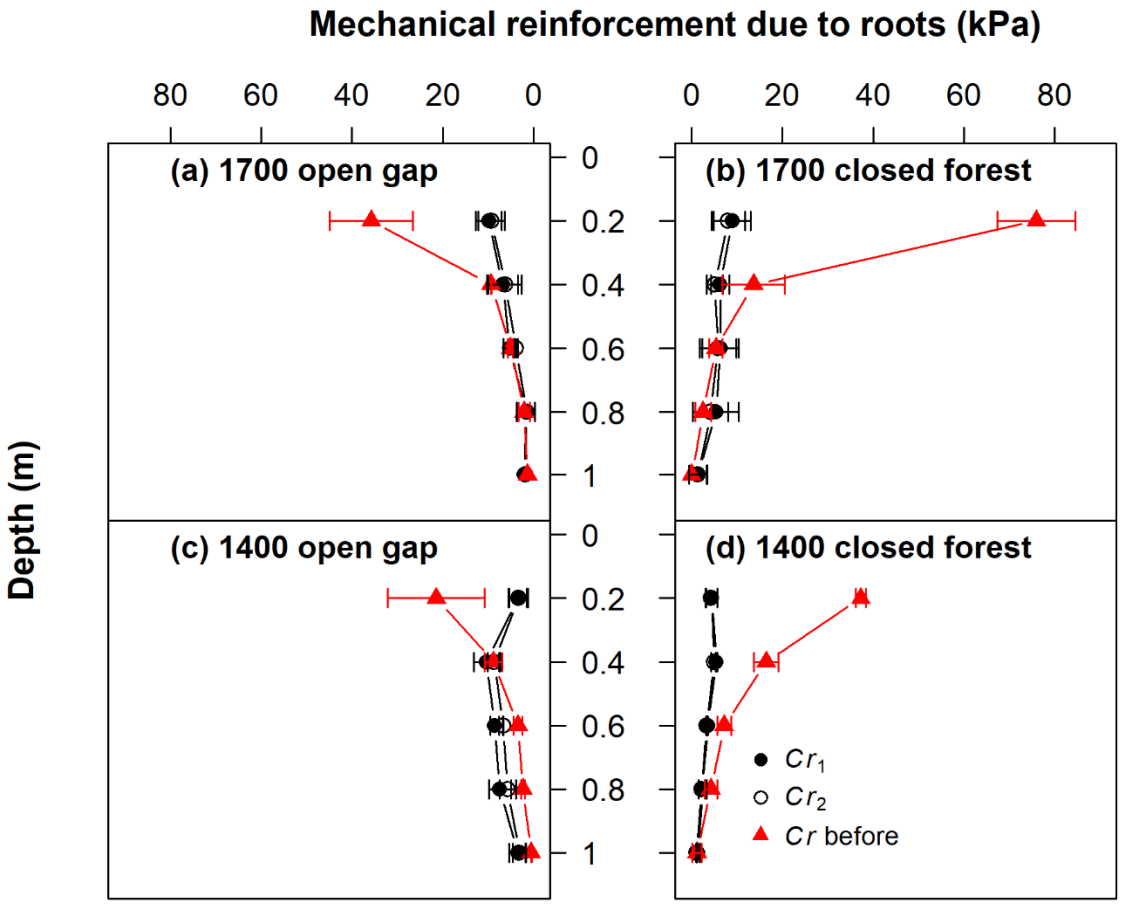

911

912 Figure 5

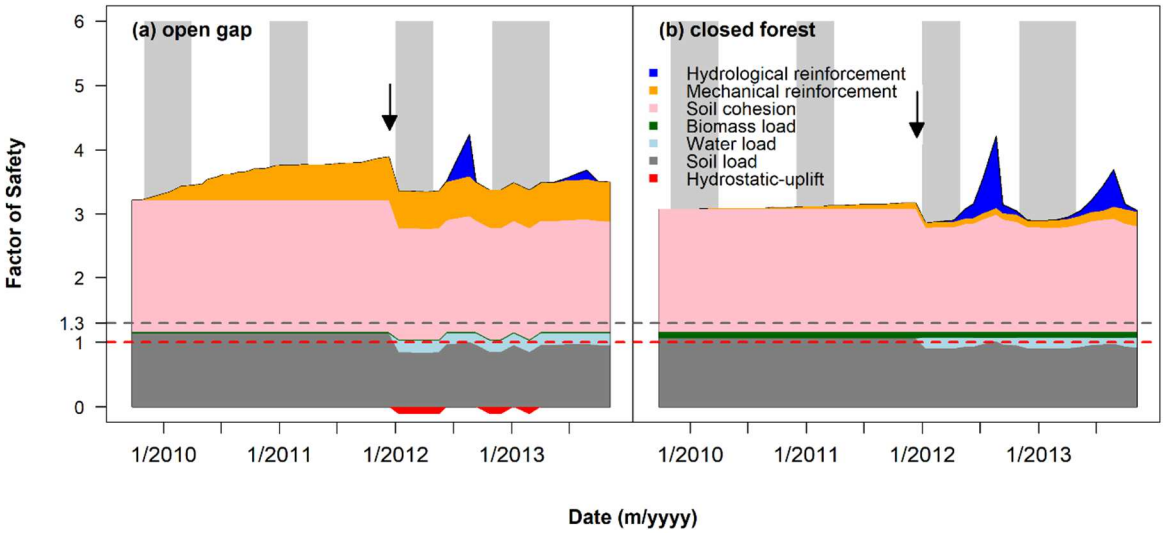

913